J Mater Sci (2007) 42:5335–5339
DOI 10.1007/s10853-006-0888-8

Effect of Nd substitution on structure and magnetic properties of $Nd_xDy_{3-x}Fe_5O_{12}$ garnet powders

Liming Yu · Jiujing Wang · Shixun Cao · Shujuan Yuan · Jincang Zhang

Received: 13 November 2005 / Accepted: 24 August 2006 / Published online: 29 March 2007

Abstract The properties of light rare earth Nd substitution for heavy rare earth Dy in $Dy_3Fe_5O_{12}$ (DyIG) garnet ferrite have been studied. The $Nd_xDy_{3-x}Fe_5O_{12}$ (x = 0, 0.25, 0.5, 0.75 and 1) (Nd:DyIG) garnet powders were prepared by sol–gel autocombustion followed by heat treatment. The structure and the magnetic properties of the annealed powders were measured with X-ray diffraction (XRD), the Fourier Transform Infrared (FT-IR) and the Physical Properties Measurement System (PPMS) techniques. The experimental results indicate that a single Nd:DyIG garnet phase structure can be obtained after the samples annealed above 800 °C. With the Nd substitution content increasing, the average lattice constants of the sample, the *a–d* super-exchange interaction strengthens and the magnetization of unit cell increase. The maximum saturation magnetization is 13.86 emu/g for x = 1, and coercive force is about 136 Oe, for x = 0.75. The reason of increasing in magnetization with Nd substitution is also discussed.

Introduction

Magneto-optical (MO) materials have now been applied to the devices for magneto-optical storage system and optical communication system, which attracts many researchers' interests. Rare earth iron garnets, with the chemical formula $R_3Fe_5O_{12}$, exhibit MO properties suitable for applications in the MO devices because of their large Faraday rotation (FR) and good corrosion resistance [1–8]. Due to DyIG ferrite has notable MO effect, many efforts have been made to improve its MO properties by doping method, and have got many useful results. For examples, the substitution of diamagnetic Bi^{3+} and Pb^{2+} ions and some lighter rare-earth ions like Ce^{3+} and Pr^{3+} strongly enhance the MO activity in the wavelength range 0.4–2 μm [9–12]. It has been found that (Bi,Ga):DyIG and (Ce,Ga):DyIG films have large MO effects[13]. But, the study on the light rare earth Nd substitution of the heavy rare earth Dy in DyIG ferrite has not been reported.

It is known that the configuration of the unfilled electron shell of the light rare earth Nd atom in ground state is $4f^3$ (three spins parallel each other) and heavy rare earth Dy atom in ground state is $4f^9$ (seven spins parallel, two spins anti-parallel). Thus, the unpaired spin electrons and the interaction between electronic spin and orbit, and the array directions of the magnetic ions in an unit cell would greatly affect the magnetic properties of the garnet. In the present work, the precursors of Nd:DyIG garnet powders are prepared by sol-gel combustion followed by heat treatment, and the structures and magnetic properties of the annealed powder with different Nd content are analyzed. The reason of enhancement in magnetization and the effects on the structure and magnetic properties of the substitution Nd for Dy in DyIG, and the correlation between them are studied.

Experimental

Stoichiometric (Nd:DyIG) amount of the starting materials including neodymium nitrate, iron nitrate and citric acid monohydrate of a certain molar ration were dissolved in distilled water, respectively. The stoichiometric amount of

L. Yu (✉) · J. Wang · S. Cao · S. Yuan · J. Zhang
Department of Physics, Shanghai University, Shanghai 200444, P.R. China
e-mail: lmyu@mail.shu.edu.cn

dysprosium oxide was dissolved in diluted nitric acid. Then the solution was mixed and dissolved into the citric acid solution. After a few minutes of moderate heating and stirring, a certain amount of ethylendiamine solution was added until pH value of the solution was about 6–7. The solution was slowly evaporated till combustion through continuously heating. Then, the powders were annealed at 600, 700, 800, 900 and 1000 °C for one hour, respectively. The heating rate was 3 °C/min.

The effect of Nd substitution on the structure and magnetic properties of $Nd_xDy_{3-x}Fe_5O_{12}$ (x = 0, 0.25, 0.5, 0.75 and 1) (Nd:DyIG) garnet powders are investigated on the samples annealed at 1000 °C for one hour. The structures of the powders were identified by X-ray diffraction (XRD, Model D/max-2500) using Cu-Kα radiation with a scanning speed of three degrees per minute in the range of 2θ = 10–90°, the Scanning Electron Microscope (SEM, Model S-570) and the Fourier Transform Infrared (FT-IR, Model AVATAR 370) in the range of 400–4000 cm^{-1}. The magnetic properties were analysed by Physical Properties Measurement System (PPMS-9) at 300 K. The maximum external magnetic field was 10000 Oe.

Results and discussion

XRD patterns and SEM analysis

Figure 1 shows the XRD patterns of $NdDy_2Fe_5O_{12}$ garnet powders annealed at different temperature. The major diffraction peaks are marked at 1000 °C. The XRD patterns indicate that the powder is a mixture of $DyFeO_3$ (PDF#47-0069), $FeNdO_3$ (PDF#25-1149) and Fe_2O_3 (PDF#33-0664)

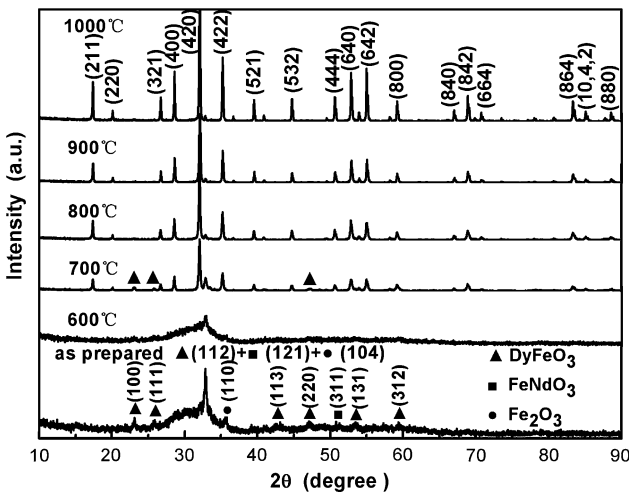

Fig. 1 XRD patterns of the $NdDy_2Fe_5O_{12}$ garnet ferrite powders annealed at different temperature. There, ▲ $DyFeO_3$; ■ $FeNdO_3$; • Fe_2O_3

after sol-gel autocombustion. An amorphous phase presents at about 600 °C and, after the powder is annealed at 700 °C, the garnet phase is almost formed. Although some $DyFeO_3$ still exist at this stage, above 800 °C, there is only a single-garnet phase structure. Therefore, the $NdDy_2Fe_5O_{12}$ garnet formation process should be written as follows:

$$2DyFeO_3 + FeNdO_3 + Fe_2O_3 \longrightarrow \text{about.800}^{o}\text{C} NdDy_2Fe_5O_{12} \quad (1)$$

Figure 2 shows the SEM images of $NdDy_2Fe_5O_{12}$ precursor annealed at 600, 700 °C, respectively. An amorphous image can be seen from Fig. 2(A). No obvious crystallites could be identified. After the powder annealed at 700 °C, there are many tiny crystallites to appear (Fig. 2(B)). These images are coincident with the XRD patterns of Fig. 1.

Figure 3 shows the XRD patterns of $Nd_xDy_{3-x}Fe_5O_{12}$ garnet powders annealed at 1000 °C for x = 0–1. The results indicate that the peak positions of diffraction angle (400), (420) and (422) have a small shift toward the lower angle part as Nd^{3+} ions increasing in the 24c sites. When x increases from 0 to 1, the three peak-positions shift about 0.16° for (400), 0.18° for (420) and 0.20° for (422), respectively. In order to know the detail changes in the structure, we use Jade 5 software (materials data, Inc.) to compute the average lattice constants from the locations of six low-angle peaks with known Miller indices ([211], [220], [321], [400], [420], [431]). The results are shown in Fig. 4, which indicates that the average lattice constants increase from 12.4138 Å to 12.4805 Å, corresponding to $Nd_xDy_{3-x}Fe_5O_{12}$ (x = 0) and $Nd_xDy_{3-x}Fe_5O_{12}$ (x = 1).

FT-IR spectra analysis

The FT-IR spectra analysis is performed to investigate the correlation between the structures and magnetic properties for $Nd_xDy_{3-x}Fe_5O_{12}$. Figure 5(A) and Table 1 show the experimental results of FT-IR spectra of $Nd_xDy_{3-x}Fe_5O_{12}$ powders annealed at 1000 °C in the range of 400–800 cm^{-1} for x = 0–1. It presents that the Nd substitution for Dy in DyIG garnet causes the three absorption bands of K1, K2 and K3 change. These three bands should correspond to the stretching vibrations of the tetrahedral metal-oxygen band, the vibrating of the octahedral metal-oxygen band, and the dodecahedral metal-oxygen band, respectively [14]. The K1, K2 and K3 bands shift towards lower frequency side as the Nd content increases (as shown in Fig. 5(A)), which means the increase in bond length. That is, the bond lengths of the $Fe^{3+} - O^{2-}$, $Nd^{3+} - O^{2-}$ and $Dy^{3+} - O^{2-}$ among the 24c, 16a and 24d sites increase. Table 1 gives the shift values of wave numbers for 24c, 16a and 24d sites from

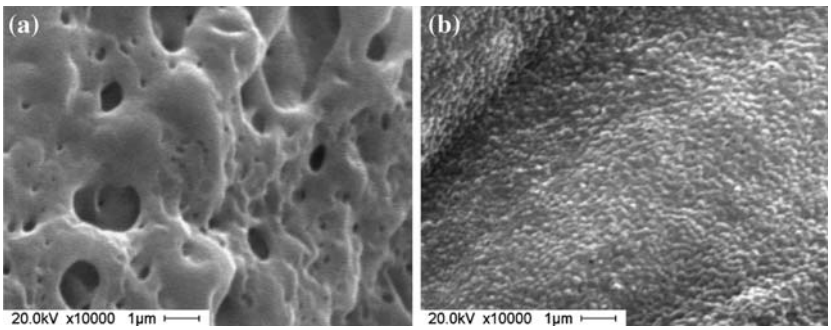

Fig. 2 SEM images of the $NdDy_2Fe_5O_{12}$ precursor annealed at (**A**) 600 °C, (**B**) 700 °C, respectively

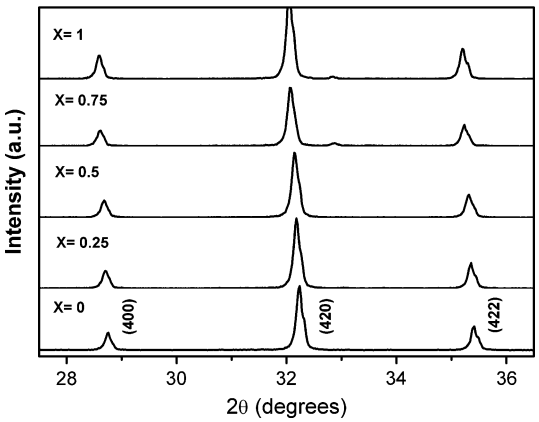

Fig. 3 XRD patterns of $Nd_xDy_{3-x}Fe_5O_{12}$ garnet powders annealed at 1000 °C for x = 0–1

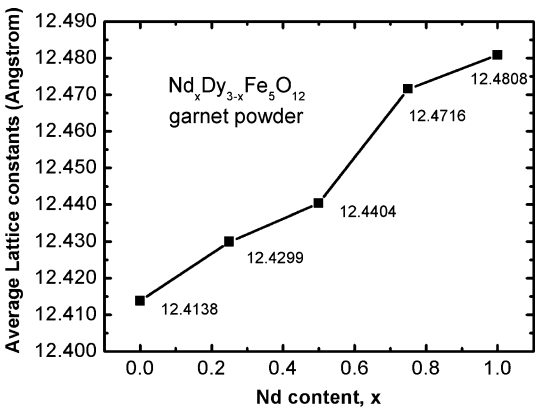

Fig. 4 The average lattice constants vs. Nd content, x for Nd:DyIG ferrite powders annealed at 1000 °C

x = 0–1 are 8.04, 9.66 and 7.60 cm^{-1}, respectively. In which, the change of wave number in 16a site is greater than that of in 24c and 24d sites corresponding to the Nd substitution increase. So, it is reasonable to deduce that the wave number changes will affect the super-exchange interaction of magnetic ions in different sites. Thus, we draw the curves of the variation of the differences between K1 and K2; K1 and K3; K2 and K3 with respect to Nd substitution (as shown in Fig. 5(B)). The results show that the (K1–K2) value increases, the (K2–K3) value decreases and the (K1–K3) value has no obvious changes as Nd substitution increases. As described in the above, the decrease in distance between ions means the ion bond shortens, the vibration frequency and the wave numbers increase. Therefore, (K1–K2) value increase means the decrease of the distance between a and d sites. This may strengthen the a–d super-exchange interaction. Similarly, the decrease of the (K2–K3) value means the increase of the distance between a–c sites. But, there is no obvious change in the (K1–K3) value. Therefore, according to the theory of super-interaction, the magnetization of unit cell will increase because the maximal and second super-interaction lies in a–d sites and d–c sites for RIG garnet ferrite. The experimental results of the magnetic measurement have proved the above prediction (as shown in Fig. 6).

Magnetism analysis

Figure 6 shows the variations of the saturation magnetization and coercive force of the annealed powders at 300 K vs. Nd content, x. The maximum saturation magnetization reaches 13.86 emu/g for x = 1. This value is greater than that of Al-substituted Bi-DyCoIG nanoparticles (8.4 emu/g) [15]. As discussed in the above, the magnetic properties of the garnet ferrite Nd:DyIG are determined by three major super-exchange interactions of $Fe^{3+}(a) - O^{2-} - Fe^{3+}(d)$, $Fe^{3+}(d) - O^{2-} - Nd^{3+}(c)$ and $Fe^{3+}(d) - O^{2-} - Dy^{3+}(c)$. Then, the molecular saturation magnetization can be given by [16]:

$$M_{\mathrm{RIG}} = (M_d - M_a) - M_c \quad (T > T_{\mathrm{comp}}) \tag{2}$$

According to the atomic orbital theory and Hund's principle, the configuration of the unfilled electron shell of the light rare earth Nd atom in ground state is $4f^3$ (three spins parallel each other) and heavy rare earth Dy atom in ground state is $4f^9$ (seven spins parallel, two spins anti-parallel). According to the principles of the super-exchange interaction, the magnetic moments of the $Nd^{3+}(c)$ ion are parallel to the magnetic moments of the $Fe^{3+}(d)$ ion, while the magnetic moments of the $Dy^{3+}(c)$ ion are anti-parallel to the magnetic moments of $Fe^{3+}(d)$ion. Because the net

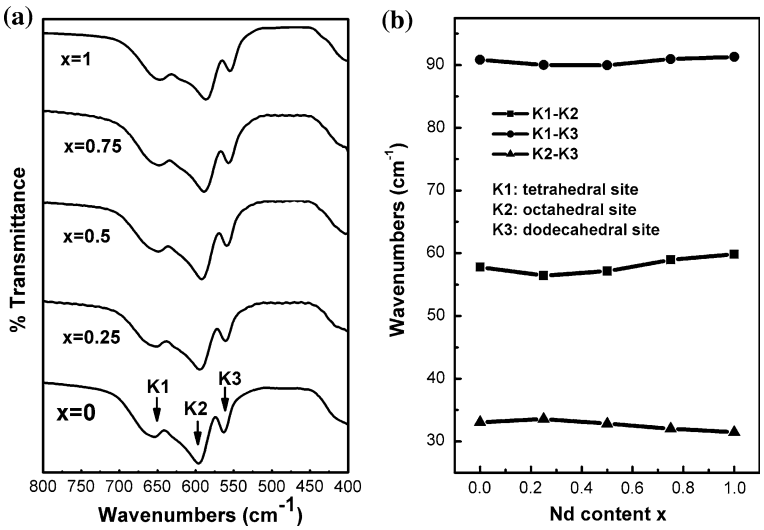

Fig. 5 (**A**) FT-IR spectra of $Nd_xDy_{3-x}Fe_5O_{12}$ powders annealed at 1000 °C in the range of 400–800 cm^{-1} for Nd content x = 0–1, (**B**) Curves of the variation of the differences between K1 and K2; K1 and K3; K2 and K3 with respect to Nd substitution content

Table 1 The positions of FT-IR absorption bands K1, K2 and K3 of Nd:DyIG garnet ferrite powders in the range of 400–800 cm^{-1} as a function of Nd content, x

Peaks (cm^{-1})	x = 0	x = 0.25	x = 0.5	x = 0.75	x = 1
K1	653.96	650.93	649.09	647.87	646.36
K2	596.18	594.50	591.96	588.94	586.52
K3	563.11	560.92	559.12	556.91	555.07

molecular saturation magnetic moments of the Fe^{3+} ions between d-site and a-site are 5.0 μ_B, therefore, the ferrite magnetization could be expressed by following equation:

$$M_{\text{Nd:DyIG}} = 5\mu_B + x \cdot M_{\text{Nd}^{3+}} - (3-x) \cdot M_{\text{Dy}^{3+}} \quad (T > T_{\text{comp}}) \tag{3}$$

That is, the saturation magnetization of Nd:DyIG will increase with the $Nd^{3+}(c)$ substitution. This prediction is coincident with the experimental results.

The variations of the coercive force of the annealed powders with Nd content are not very large. The results show that the coercivity of the annealed powders increases at first, and then decreases with the substitution content increase. The maximum coercivity value is 136 Oe for x = 0.75. The reason may be due to the increase in the crystal field anisotropy as the bigger diameter Nd ions are introduced.

Conclusions

Nd:DyIG powders can be prepared by sol-gel autocombustion followed by heat treatment. The powders have a single-garnet phase structure after the precursor annealed above 800 °C. The average lattice constants and the unit cell volume increase as Nd content increases. The analysis of FT-IR spectra and the experimental data indicate that the light rare earth Nd^{3+} ion substitution for heavy rare earth Dy^{3+} ion will strengthen the a–d super-exchange interaction, and increase the magnetization of the unit cell. The maximum saturation magnetization of the sample reaches 13.86 emu/g for x = 1. The maximum coercivity value is 136 Oe for x = 0.75. The MO effect of the Nd:DyIG powder will be discussed in the other paper.

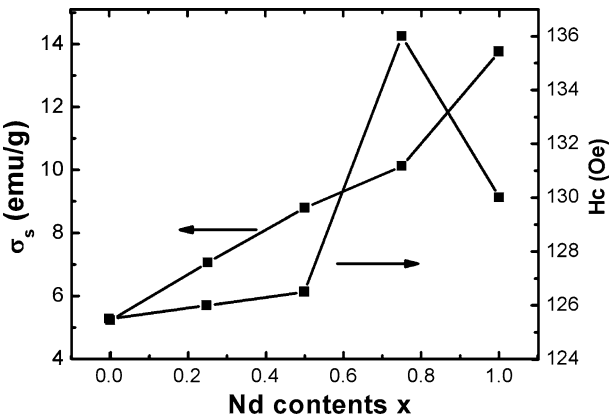

Fig. 6 The variations of the saturation magnetization and coercive force of the annealed powders at 300 K vs. Nd content, x

Acknowledgements This work is supported by the National Foundation of the Natural Science of China (No.10504019) and the Shanghai Leading Academic Discipline Program (No.T0104).

References

1. Hansen P (1990) J Magn Magn Mater 83:6
2. Papakonstantinou P, Teggart B, Atkinson R (1996) J Magn Magn Mater 163:378
3. Eppler WR, Kryder MH (1995) J Phys Chem Soleds 56:1479

4. Laulajainen M, Paturi P, Raittila J, Huhtinen H et al (2004) J Magn Magn Mater 279:218
5. Krumme JP, Doormann V, Willich P (1985) J Appl Phys 57:3885
6. Martens JW (1986) J Appl Phys 59:3820
7. Ostorero J, Guillot M, Aritiniom W (1988) IEEE Trans Magn 24:2560
8. Hansen P, Witter K, Tolksderf W (1983) Phys Rev B 27:6608
9. Krumme JP, Doormann V, Hansen P, Baumgart H, Petruzello J, Viegers MPA (1989) J Appl Phys 66:4393
10. Wemple SH, Dillon JF Jr, Van Uitert LG, Grodkiewicz WH (1973) Appl Phys Lett 22:331
11. Zhang F, Xu Y, Yang J, Guillot M (2000) J Phys: Condens Mater 12:7287
12. Teggart B, Atkinson R, Salter IW (1998) J Phys D: Appl Phys 31:2442
13. Shono K, Kuroda S, Alex M, Ogawa S (1990) J Magn Magn Mater 88:205
14. Modi KB, Vara RP, Vora HG, Chhantbar MC, Joshi HH (2004) J Mater Sci 39:2187
15. Kim T-Y, Yamazaki Y (2004) IEEE Trans Magn 40:2793
16. Guillot M, Feldmann P, Le Gall H, Fadly M (1978) IEEE Trans Magn Mag 14:909